Characterization and modeling of cooling and drying of pellets for animal feed

Charlène Lambert, Julien Cartailler, Sandy Rouchouse, Giana Almeida, Francis F. Courtois

Characterization and modeling of cooling and drying of pellets for animal feed

Charlène Lambert[a], Julien Cartailler[a], Sandy Rouchouse[b], Giana Almeida[a], Francis Courtois[a,*]

[a] *UMR Ingéniérie Procédés Aliments, AgroParisTech, Inra, Université Paris Saclay, 91300 Massy, France*
[b] *Tecaliman (technical center), F-44316 Nantes Cedex 3, France*

Abstract

The process used to produce pellets for animal feed, especially the drying-cooling step, has not been extensively explored in the literature. However, with the increased industrial use of adjustable-speed drives to reduce fan energy consumption, the need for reliable simulation models has increased. In this work, different formulations of pellets were characterized and both their drying and drying-cooling kinetics were modeled. In comparing the results of the simulations with experimental results, the observed discrepancies were similar to the experimental uncertainties, indicating that our prediction tools yielded imperfect but acceptable results both in the thin-layer and deep-bed drying configurations. Furthermore, the approach centered on drying kinetics was also able to predict drying-cooling kinetics. This work suggests that one simple EMC equation, without temperature dependency, may correctly fit the behavior of several kinds of pellets and be sufficient for accurate simulations. The overall approach may be easily applied to many other kinds of pellets.

Keywords: cooling, drying, pellets, animal feed, characterization, model

1. Introduction

The process by which pellets are manufactured consists of several steps: grinding, weighing raw materials, mixing, pelleting to agglomerate small particles into larger ones, cooling, and conditioning. Despite its economic importance, this process has been largely ignored in the literature, with only a few exceptions. The limited research conducted to date has mainly focused on the effect of pellet formulation on the manufacturing process (Wood, 1987; Thomas & van der Poel, 1996; Thomas et al., 1998; Hemmingsen et al., 2008), or the conditioning (Thomas et al., 1997) or pelleting (Thomas et al., 1997; de Blank et al., 1997) steps of the process.

*Francis Courtois
Email addresses: charlene.lambert@agroparistech.fr (Charlène Lambert), julien.cartailler@agroparistech.fr (Julien Cartailler), s.rouchouse@tecaliman.com (Sandy Rouchouse), giana.perre@agroparistech.fr (Giana Almeida), francis.courtois@agroparistech.fr (Francis Courtois)

Even if cooling is not one of the most energy-consuming steps of this process, industrial investment has recently focused on the use of adjustable-speed drives to reduce fan energy consumption. This technology conserves energy by adapting air flow to the actual needs of the pellets at any given time. However, for most of these coolers, there is no real-time feedback between measurements of pellet characteristics (e.g., humidity, temperature) and processing parameters. Ideally, measurements of air humidity taken from a cooler's exhaust could be used to optimize the drying-bed height or fan velocity. Moreover, the lack of automatic control of the cooling process may lead to overdrying of pellets, resulting in higher energy consumption and cracks in the pellet surface which affect their durability (Thomas et al., 1997). Hence, precise control of this step of the process is of the utmost importance for the animal-feed industry in order to optimize energy consumption and ensure product quality. For this reason, the French Environment and Energy Management Agency (ADEME) funded the OPSERA project ("Optimizing Dryer-Cooler Performance for Animal Feed"), which aimed to optimize the drying-cooling process in real time using an advanced control algorithm. The control scheme centers on the estimation of pellet moisture content by a *smart sensor*, which utilizes observation/estimation techniques based on a dynamic simulation model of the drying-cooling process. This paper describes the characterization and modeling of the drying and cooling of pellets as required for the real-time estimation of their moisture content.

In some respects, the lack of scientific attention given to the cooling process (with the exception of (Kelley et al., 1990; Maier & Bakker-Arkema, 1992; Maier et al., 1992)) is surprising, given that the cooling operation is also a drying one: the cold air blown is used to decrease both pellet moisture content and temperature. Drying/cooling thus represents a crucial final step in pellet production. However, the strong coupling between cooling and drying phenomena makes the operation difficult to optimize in the absence of accurate simulations. Over two decades ago, a drying-cooling model was developed by (Maier & Bakker-Arkema, 1992) and its simulations were validated at a pilot scale. However, this model was only able to predict the trend of moisture and temperature effects on cooler performance (Kelley et al., 1990; Maier & Bakker-Arkema, 1992; Maier et al., 1992) and did not accurately predict moisture loss and temperature in pellets (up to 60% deviation was observed between experimental and simulated data). Hence, what is needed today is a more accurate model that can control an industrial cooler and predict the effects of changes in pellet formulation on operating conditions. Ideally, such a model would also be able to take into account changes in pellet composition, as pellet recipes are changed continuously in response to variations in the cost of ingredients (soya, corn, etc.). These changes are likely to affect drying-cooling performance and represent a challenge to model development.

The purpose of this work was to develop a convective drying-cooling model that could be implemented in two versions: 1) an unsteady-state version, in order to control process parameters, and 2) a steady-

state version, in computer-aided engineering (CAE) software. In a recent work discussing classical modeling approaches of convective drying processes (Lambert et al., 2015a), it was argued that the main characteristics of a successful model should be a low computational requirement and a wide range of validity. Simulation of the drying or drying-cooling operation should not last longer than a few seconds, and the model should also have multi-product compatibility and extrapolation capability. It should be able to simulate all classical drying and drying-cooling conditions. In addition, it should allow the late addition of new products or at least new formulations without the need to modify the equations. Thus, parameters of the model should have a physical meaning and should be calculated with correlations, experimentally measured, or identified by reverse methods (Lambert et al., 2015a).

The aim of our model was to predict the final moisture content of pellets and the energy consumption of the drying-cooling process. However, obtaining reliable drying-cooling kinetics is difficult, especially in the thin-layer configuration. Hence, we decided to first focus on a drying-only model. We then attempted to validate this model using deep-bed cooling-drying kinetics.

2. Materials and methods

There is almost an infinite number of formulations of animal feed pellets. This study focused on the experimental characterization of two formulations, with various recipes and pelleting conditions. Water activity and effective moisture diffusivity were identified using DVS data and drying kinetics, respectively.

2.1. Origin of the pellets

The two formulations of animal feed pellets studied were pellets for chickens (P4C) and for rabbits (P4R). In the latter case, we studied two different geometries of the same composition (same raw materials and recipe). These were designated P4R - 2.5 mm and P4R - 4 mm. All formulations had a cylindrical shape. Raw seed composition and dry matter composition of both pellet formulations are given in tables 1 and 2, respectively. For the pelleting process, ingredients were mixed with steam in a conditioner then pelleted in a press. The temperatures of the pellets at the press outlet were 84°C (P4C), 87°C (P4R - 2.5 mm), and 83°C (P4R - 4 mm). The pellet moisture content at the press outlet was 0.204 d.b. (P4C), 0.211 d.b. (P4R - 2.5 mm), and 0.202 d.b. (P4R - 4 mm). For each formulation and geometry, 2.5-kg samples of pellets were vacuum-packed in plastic boxes and later stored in a cold room.

2.2. Moisture content measurement

Pellet moisture content was measured according to the French AFNOR norm NF V 18-109, before thin-layer and deep-bed drying and after thin-layer drying. The pellets were first ground using a water-cooled

miller (IKA WERKE KM 20). The measurement method assumes a weight loss of 5.00 g (± 0.05 g) of pellet powder during a 4-hour stay in a 103°C oven. Samples were then placed in a desiccator for at least 1 hour before being weighed. The moisture content was averaged over three samples.

2.3. Geometry measurement

Apparent density of pellet dry matter was measured using Fontainebleau sand. Real density of pellet dry matter was determined using an air pycnometer (ACCUPYC 1330). Pellet dimensions were measured using two methods: a manual approach using a caliper and an automated approach based on image analysis (using a flatbed scanner and *ImageJ* software). Porosity of the bed was determined according to equation 1.

$$\varepsilon = \frac{\rho_{dm}^{real} - \rho_{dm}^{ap}}{\rho_{dm}^{r}} \tag{1}$$

where ε is the bed porosity (decimal), ρ_{dm}^{real} the real density of the dry matter ($kg.m^{-3}$) and ρ_{dm}^{ap} the apparent density of the dry matter ($kg.m^{-3}$).

2.4. Sorption isotherm measurement

Isothermal analyses were performed using a DVS Intrinsic apparatus (Surface Measurement Systems, London, UK). An ultra-sensitive micro-balance enabled the measurement of mass variations as small as 1 part per 10 million. First, samples were ground using a water-cooled miller (IKA WERKE KM 20). Approximately 10 mg of each sample was inserted in the pan. In the DVS device, a constant flow of nitrogen gas was mixed with a preset amount of water vapor. Nitrogen then passed through the chamber to maintain the desired relative humidity level, ± 0.5%. All sorption cycles started with 0% relative humidity (RH). The dry matter was determined from values obtained after the plateau was reached. Isotherms were measured at two different temperatures for P4Cs (25°C and 40°C) and at 25°C for P4Rs; P4R measurements were performed in duplicate. Adsorption/desorption cycles of relative humidity (RH) looped from 0% up to 90% then back down to 0%, by steps of 10% RH. In experiments at 40°C, 92.3% RH (± 0.4% RH) was measured instead of 90% RH due to inadequate performance of the RH control loop. All reported results were based on actual measured RH values (which occasionally differed from target values). The instrument maintained a constant RH until the change in sample moisture content was less than 0.002% per minute over a 10-min period. This threshold value was obtained from Hill et al. (2009), in order to obtain a final sample moisture content within 0.1% of the equilibrium value over an extended period of time.

Equilibrium moisture content (X_{eq}) and relative humidity (RH) / water activity (a_w) data were fitted using a modified Henderson equation (equation 2) (Henderson, 1952; Thompson, 1968) without temperature dependency and the Chung-Pfost correlation (equation 3) (Chung & Pfost, 1967). The Henderson equation

is one of the five equations recommended by ASAE Standard D245.6 for fitting sorption data from several agri-food materials (ASAE, 2007). The Chung-Pfost correlation was used by (Maier & Bakker-Arkema, 1992) and (Brook & Foster, 1981) but, as will be discussed later, this equation (3) cannot guarantee that when $X_{eq} = 0$ then $a_w = 0$, which is a major flaw for simulators.

$$a_w = 1 - exp\left(-p_1 \cdot (X_{eq})^{p_2}\right) \tag{2}$$

$$X_{eq} = p_1 - p_2 \cdot ln\left(-p_3 \cdot (\Theta + p_4) \cdot ln\left(a_w\right)\right) \tag{3}$$

where p_1 - p_4 are constants that need to be identified using experimental data, X_{eq} is the equilibrium moisture content (% d.b.), and Θ is the product surface temperature (°C).

2.5. Drying experiment

Pellets were dried using two different protocols: a conventional hot-air drying approach (i.e. several thin layer kinetics and one deep bed kinetic) and a drying-cooling method (deep-bed kinetics only). Measurements of thin-layer kinetics were performed in triplicate. For both methods, experimental data were recorded using an automated pilot dryer located in an AgroParisTech/INRA drying laboratory (Massy, France) under constant conditions (see below).

2.5.1. Description of the drying pilot

A schematic of the drying pilot is given in figure 1. In this pilot, the air passes, from the top to the bottom, through a cylindrical drying chamber (25 cm in diameter and 28 cm in height). The following variables were recorded every minute (with an OPTO22 SNAP-PAC-EB2 data logger):

- inlet and outlet air temperatures (with T-type thermocouples and platinium probes) and relative humidities (with VAISALA 135Y and ROTRONIC HF532-HC2 probes);
- inlet air velocity (using an ANNUBAR ANR-73 Pitot tube and a FURNESS FCO-53 differential pressure sensor);
- mass of the product (with a METTLER PE 16 discontinuous weighing system with air bypassed).

The precision of measurements of mean moisture content was estimated for each formulation of pellets by repeating measurements of thin-layer kinetics. The following uncertainties were determined:

- P4C: ± 0.015 d.b. (σ = 0.005 d.b.);

- P4R - 2.5 mm and P4R - 4 mm: ± 0.018 d.b. ($\sigma = 0.06$ d.b.).

For measurements of relative humidity and temperature in the pilot dryer, the following uncertainties (using $\pm 3\,\sigma$) were determined:

- Inlet air temperature: ± 1.5°C ($\sigma = 0.5$°C);
- Outlet air temperature: ± 2.5°C ($\sigma = 0.8$°C);
- Inlet and outlet relative humidities: ± 5% ($\sigma = 1.7\%$)

However, actual deviations in measurements of outlet air temperature and relative humidity may have been greater than those estimated here, for three reasons. First, due to the intermittent nature of the mass measurement system, minor air leaks and locally reduced thermal insulation below the sieve were unavoidable. Second, it is possible that having the sensor close to the sieve introduced bias due to thermal radiation. Finally, due to the depth of the beds, air flow below the sieve was less homogeneous. Because of this, the outlet air temperature may have been slightly underestimated. In addition, the response time of the relative humidity sensor (45 s) was not negligible compared to the sudden variations in relative humidity in the first minutes of the drying process. As a consequence, a comparison of experimental and simulated data during this initial period was undertaken very carefully (see discussion).

2.5.2. Drying and drying-cooling protocols

Drying method. Thin-layer and deep-bed drying kinetics were recorded using P4Cs and P4Rs (P4R - 4 mm and P4R - 2.5 mm). About 200 g (thin layers) and between 2.5 to 5 kg (deep beds approximately 0.10- to 0.20-m high) of pellets were introduced into the dryer. Operating conditions of the dryer are summarized in table 3.

Drying-cooling method. As stated in the introduction, it is quite difficult to precisely control the initial conditions of the pellets entering the drying-cooling experiment. It takes considerable effort to warm up the pellets without drying them and then transfer them to the dryer without the premature loss of water or heat. Even when this can be done, it is extremely challenging to then obtain accurate measurements of the actual initial product temperature and moisture content at the beginning of the drying-cooling step. In this work, no reliable data could be obtained for thin-layer drying-cooling kinetics, hence, the only drying-cooling data available were for the deep-bed drying kinetics of P4Cs. About 5 kg of pellets were vacuum-packed using a vacuum heat sealer (MULTIVALUED GASTRONOMIC) and pouches composed of low-density polyethylene (LEXINGTON). Packing pellets in a vacuum-sealed bag limited pellets' contact with air and minimized mass transfers during preheating. The pellets and the sieve were then pre-heated as follows:

- The sieve of the dryer was preheated to about 100°C using a heat gun (METABO H 1600) in order to be at nearly 80°C at the beginning of the experiment;
- Pellets, in their vacuum-sealed bags, were pre-heated in a 100°C oven for one hour. The core temperature of the pellets was about 60 - 70°C when taken out of the oven.

Pellets were then introduced into the drying zone after stabilization of the dryer's operating conditions (tested conditions are listed in table 3). A sub-sample was withdrawn for moisture content measurement. The initial temperature of the pellets was initially estimated through the use of an infrared thermometer, but these measurements were not used because of suspected bias. A better estimate was obtained from the recorded outlet air temperature after two minutes of drying-cooling.

2.6. Identification of D_{eff}

This study continues previous work that discussed three different approaches for the identification of effective moisture diffusivity D_{eff}. (Lambert et al., 2015b). Here, these three strategies were used for the identification of the effective moisture diffusivity of pellets as summarized in table 4.

As a reminder, the classical strategy used in food drying consists of four steps:

1. Measure in the laboratory the accessible properties of the product (water activity, heat capacity, geometry, and porosity);
2. Collect experimental measurements of thin-layer drying kinetics under constant air drying conditions over a wide range of air temperatures;
3. Identify the effective moisture diffusivity coefficient by fitting a model to these thin-layer drying kinetics (using variations of recorded product moisture content);
4. Validate the model using some thin-layer (using product moisture content) and/or deep-bed drying kinetics (using product moisture content and possibly output air moisture and temperature).

This strategy was used to identify the effective moisture diffusivity of P4Rs - 2.5 mm. The validation set contained both thin-layer and deep-bed drying kinetics. As explained in a previous study (Lambert et al., 2015b), in this strategy, the mass variation of the product is the only experimental data used to identify the effective moisture diffusivity. However, using only mass-transfer-related information is problematic since, in drying, this transfer is strongly coupled to energy change. In a deep-bed experiment, though, inlet and outlet air temperatures and relative humidities may be recorded in order to provide energy-related data (Lambert et al., 2015b). By providing data on both heat and mass transfers, an approach based on deep-bed drying kinetics brings far more information to the identification procedure compared to those based on several measurements of thin-layer kinetics. With this in mind, the two other developed strategies were

derived from the classical one, but with a major difference: effective moisture diffusivity was identified using deep-bed drying kinetics as opposed to thin-layer kinetics Lambert et al. (2015b). In the first approach, the identification set contained drying kinetics from a single deep-bed setup, obtained at a high temperature (90°C). The validation set contained both thin-layer drying kinetics and a set of deep-bed drying-cooling measurements of P4Cs. With the second approach, two sets of data were obtained for deep-bed kinetics, one at 40°C and one at 80°C, to identify effective moisture diffusivity of P4Rs - 4 mm. The validation set was obtained from a thin-layer configuration.

For all identification strategies, operating conditions of the identification set are summarized in table 4 and operating conditions of the validation set are in table 3. The Abud correlation (Abud-Archila et al., 2000) was used to find the effective moisture diffusivity (equation 4):

$$D_{eff} = exp\left(-d_1 + d_2 \,.\, X \,.\, Tp\right) \tag{4}$$

where d_1 and d_2 are constants that are optimized to force the simulation to best fit the experimental data.

3. Modeling of drying-cooling

In order to develop a versatile food-drying simulation, we selected the following compromise among the different approaches, published in a previous work (Lambert et al., 2015a), and considered some major assumptions. A convective drying model was created for both deep-bed and thin-layer configurations. One usually treats the deep bed as a series of thin layers for which the only transfer occurs between air and grain, and a thin layer as an equivalent single (average) particle. Moreover, deep-bed drying involves energy and mass transfers in the air, after each thin layer crossing (Courtois, 1991).

3.1. Heat and mass balances

3.1.1. For the particles

The following assumptions were considered for the particles:

- Ideal geometry (infinite cylinder or spherical shape) with negligible shrinkage or swelling;
- Isotropic behavior (heat and mass transfers only in the radial direction);
- Negligible heat conduction between particles;

The heat and mass Biot values (Bi_h and Bi_m) were, respectively, between 0.1 and 100 and much higher than 100. Therefore, heat conduction and liquid water diffusion within the particles were considered, along

with water evaporation, heat convection, and mass convection at their surfaces (Bird et al., 2002). The heat and mass Peclet values (Pe_h and Pe_m) were much higher than 1, so a plug-type airflow and negligible pressure variation were assumed (Bird et al., 2002). Heat and mass balances for the particles, liquid water diffusion (equation 5) and thermal conduction (equation 6) phenomena were based on Fick's and Fourier's law, respectively (Bird et al., 2002).

$$\frac{dX_t^{r,\,z}}{dt} = \frac{1}{r^n} \cdot \frac{\partial}{\partial r}\left(r^n \cdot D_{eff.} \cdot \frac{\partial X_t^{r,\,z}}{\partial r}\right) \tag{5}$$

$$\frac{d\left(\rho_{dm} \cdot \left(Cp_{dm} + Cp_w \cdot X_t^{r,\,z}\right) \cdot Tp_t^{r,\,z}\right)}{dt} = \frac{1}{r^n} \cdot \frac{\partial}{\partial r}\left(r^n \cdot \lambda_{eff} \cdot \frac{\partial Tp_t^{r,\,z}}{\partial r}\right) \tag{6}$$

where X is the moisture content (d.b.), r the radial position in the particle (m), z the particle position in the height of the bed (m), t the elapsed time (s), n the shape factor (1 or 2 for cylindrical or spherical symmetry, respectively), $D_{eff.}$ the effective water diffusivity ($m^2.s^{-1}$), Tp the product temperature (K), $\lambda_{eff.}$ the effective thermal conductivity ($W.m^{-1}.K^{-1}$), ρ_{dm} the density of the dry matter ($kg.m^{-3}$) and Cp_{dm} and Cp_w the heat capacities at constant pressure of dry matter and water, respectively ($J.kg^{-1}.K^{-1}$), for the considered particle.

Temperature and moisture content within the particles were assumed to be initially uniform. In addition, boundary conditions are given in equations 7 to 10.

$$\frac{\partial X_t^{0,\,z}}{\partial r} = 0 \tag{7}$$

$$\frac{\partial Tp_t^{0,\,z}}{\partial r} = 0 \tag{8}$$

$$-\rho_{dm} \cdot \frac{\partial\left(D_{ap} \cdot X_t^{r_{max},\,z}\right)}{\partial r} = k_m \cdot \frac{M_w}{R} \cdot \left(\frac{a_w \cdot Pv_{sat.}}{Tp_t^{r_{max},z}} - \frac{HR \cdot Pv_{sat}}{Ta_t^z}\right) = \varphi_m \tag{9}$$

$$\lambda_{ap} \cdot \frac{\partial Tp_t^{r_{max},\,z}}{\partial r} = h_{glob} \cdot \left(Ta_t^z - Tp_t^{r_{max},\,z}\right) - \varphi_m \cdot \Delta H_v = \varphi_Q \tag{10}$$

where k_m is the convective mass transfer coefficient ($m.s^{-1}$), M_w the molar mass of water ($kg.mol^{-1}$), R the perfect gas constant ($J.kg^{-1}.K^{-1}$), a_w the water activity of the particle (Pa/Pa), Pv_{sat} the pressure of saturated vapor (Pa), RH the relative humidity (decimal), h_{glob} the external heat transfer coefficient including the heat transfer effectiveness by convection ($W.m^{-2}.K^{-1}$), Ta the air temperature (K), $\triangle H_v$ the

enthalpy of vaporization of pure water ($J.kg^{-1}$), φ_m the mass flux density ($kg.s^{-1}.m^{-2}$), and φ_Q the heat flux density ($J.s^{-1}.m^{-2}$).

3.1.2. For the air

A microscopic balance was created in the air after each thin-layer crossing (equations 11 and 12). Air moisture content and temperature were fixed at the inlet of the first thin layer but were not necessarily constant during a drying experiment.

$$\frac{d\left(\rho_{da} \cdot Y_t^z\right)}{dt} = -\frac{\partial\left(\rho_{da} \cdot v_a \cdot Y_t^z\right)}{\partial z} + \frac{\varphi_m \cdot a \cdot (1-\varepsilon)}{\varepsilon} \tag{11}$$

$$\begin{aligned}\frac{d(\rho_{da} \cdot (Cp_{da} + Y_t^z \cdot Cp_v) \cdot Ta_t^z)}{dt} &= -\frac{\partial}{\partial z}\left(\rho_{da} \cdot (Cp_{da} + Y_t^z \cdot Cp_v) \cdot Ta_t^z\right) \\ &\quad - \frac{a \cdot (1-\varepsilon) \cdot \varphi_Q}{\varepsilon}\end{aligned} \tag{12}$$

where ρ_{da} is the density ($kg.m^{-3}$) of dry air, a the particle specific surface area (surface area per particle volume) (m^{-1}), ε the bed porosity (decimal), Y the moisture content ($d.b.$), Ta the temperature (K), and Cp_{da} and Cp_v the specific heat capacities at a constant pressure of dry air and water vapor, respectively ($J.kg^{-1}.K^{-1}$), for the considered air.

3.2. Simulation and optimization

The dynamic system consisted of a set of six Partial Differential Equations (PDEs 5 to 10). These equations were discretized in space into a set of Ordinary Differential Equations (ODEs) using an explicit finite volume scheme to be numerically integrated with respect to both time and space by the explicit embedded Runge-Kutta Cash-Karp (4, 5) method (Galassi et al., 2009) (for stiff systems).

To quantify the quality of the model predictions, the maxima of relative errors between experimental and simulation data were calculated according to equations 13 and 14 for thin-layer and deep-bed drying kinetics, respectively, valid for any time t. The aim was to minimize the maximum relative error (MINMAX algorithm) obtained on the measurable variables using the Nelder and Mead method (also known as Downhill Simplex method) (Nelder & Mead, 1965).

$$MRE_{TL} = max\left(\left(\frac{\overline{X}_{sim}^t - \overline{X}_{exp}^t}{\overline{X}_{exp}^t}\right)^2\right) \tag{13}$$

$$MRE_{DB} = max\left(\left(\frac{\overline{\overline{X}}^{t}_{sim} - \overline{\overline{X}}^{t}_{exp}}{\overline{\overline{X}}^{t}_{exp}}\right)^{2}, \left(\frac{Ta^{t}_{out,\,sim} - T^{\,t}_{out,\,exp}}{Ta^{t}_{out,\,exp}}\right)^{2}\right) \quad (14)$$

where MRE_{TL} and MRE_{DB} are the respective maximum relative errors for thin-layer and deep-bed kinetics, $\overline{X}_{sim}$[1] and $\overline{\overline{X}}_{sim}$[2] the simulated mean moisture content (d.b.), $\overline{X}_{exp}$ and $\overline{\overline{X}}_{exp}$ the experimental mean moisture content (d.b.) for thin-layer and deep-bed kinetics, respectively, and $Ta_{out,\,sim}$ and $Ta_{out,\,exp}$ the simulated and experimental output air temperature (°C).

The model simulation required 13 parameters, each with a physical meaning. Some were measured in the laboratory (pellet dimensions and density, porosity of the bed, initial temperature and moisture content of the pellets), some were found in the literature (heat capacity, thermal conductivity, latent heat of vaporization, coefficients of heat and mass transfers by convection), and others identified by reverse methods (effective moisture diffusivity and water activity). All parameters required for the simulation (parameters of the model and numerical parameters of the solver) are summarized in table 5.

4. Results and discussion

4.1. Sorption isotherms

The sorption isotherms of two pellet formulations (P4C or P4R - 4 mm) are presented in figure 2. There was no visible effect of temperature within the [25°C - 40°C] range (see figure 2.A). In addition, the standard deviation for the desorption and adsorption isotherm data of P4Rs at 25°C was less than 0.5% between the two repetitions, demonstrating the reproducibility of our measurements. By comparing the sorption isotherms for the two formulations, one can observe that (see figure 2.B):

- when $a_w < 0.7$, pellets for chickens were more hygroscopic than pellets for rabbits, meaning that the latter pellets had fewer sorption sites available at low water activity values;
- when $a_w > 0.7$, pellets for rabbits were more hygroscopic than pellets for chickens, which is probably related to differences in the pellets' micro-porosity and composition. The water activity of mixtures is dependent on the fraction size of each ingredient (Hemmingsen et al., 2008). In particular, sugar beet pulp has a higher water-holding capacity than other ingredients at temperatures below 80°C (Hemmingsen et al., 2008; Serena & Bach Knudsen, 2007). Sugar beet pulp was present only in P4Rs, and was probably responsible for their more-hygroscopic behavior at high water activity values.

[1] $\overline{X}$ is the mean moisture content of each layer and is calculated as the volume-weighted average moisture content.

[2] $\overline{\overline{X}}$, the mean moisture content within the bed, is calculated as the mean of the mean moisture content of each thin layer.

However, it should be noted that variations in water activity had little influence on the accuracy of the drying model. We therefore disregarded discrepancies between sorption isotherm values for water activities below 0.8 in the framework of the drying or drying-cooling model simulation. As stated previously, two different correlations were used to fit the desorption isotherm data: the Chung-Pfost correlation (Chung & Pfost, 1967) and a modified Henderson correlation (Henderson, 1952; Thompson, 1968). The former correlation was used by Brook (Brook & Foster, 1981) to fit equilibrium moisture content and relative humidity data from soybeans. Maier *et al.* then showed that the identified parameters (p_1, p_2, p_3 and p_4 provided in equation 15) could be applied to different formulations of pellets for animal feed for relative humidity / water activity data between 20 and 90% (Maier & Bakker-Arkema, 1992).

$$X_{eq} = 0.375 - 0.0668 \cdot ln\left(-1.98 \cdot (\Theta + 24.6) \cdot ln\left(a_w\right)\right) \tag{15}$$

The identified parameters (p_1, p_2, p_3 and p_4) allowed for a good agreement with experimental data for water activities between 0.4 and 0.8, as shown in figure 3. However this correlation gives non-zero (negative) values of a_w when $X_{eq} = 0$, which is physically not acceptable and can cause numerical divergence during the simulations.

$$X_{eq} = exp\left(\frac{ln\left[-ln(1.0-a_w)/20.802\right]}{1.41185}\right) \tag{16}$$

Instead, the identified parameters for the modified Henderson correlation (provided in equation 16) gave acceptable results, as shown in figure 3. More specifically, good agreement with experimental data was observed for water activity values below 0.8. Contrary to what was found with the Chung-Pfost correlation, water activity values given by the modified Henderson correlation were positive or zero when the equilibrium moisture content was set to zero, which was expected. Therefore this latter correlation was preferred for drying and drying-cooling simulations.

4.2. Identification of D_{eff}

The identified values of effective moisture diffusivity D_{eff} are given in table 6 for each formulation and geometry. In the case of pellets for rabbits (P4R - 2.5 mm and P4R - 4 mm) with a shared initial recipe, it was possible to consider a single set of coefficients (d_1, d_2) for the effective moisture diffusivity of both geometries. However, generally speaking, the operating conditions of the pelleting stage drastically influenced the intrinsic thermophysical properties of the final product. Therefore it was preferable to identify the effective moisture diffusivity for each new formulation or set of pelleting operating conditions, which explains the slight differences observed between correlations of coefficients of effective moisture diffusivity

(see table 6).

4.3. Final validation using drying and drying-cooling kinetics

Mean absolute errors observed on mean moisture content and outlet air temperature are given in table 7 using the kinetics of the validation set of each pellet formulation. Mean errors of prediction for product moisture content were close to the actual uncertainties of the experimental data. Unsurprisingly, the largest errors were obtained from drying-cooling experiments in which the initial state of the pellets was known with less certainty.

The drying-cooling process was well-simulated in the case of pellets for chickens (figure 4). More experiments would probably be needed for full validation, but these results confirm that the overall approach based on drying kinetics gives acceptable results in predicting drying-cooling experiments.

The simulations also yielded acceptable results for the drying of the P4R - 4 mm pellets for rabbits (see figure 5) over the range of experimental conditions considered. The case of the P4R - 2.5 mm pellets for rabbits was distinct from the others in that an identification set of thin-layer, instead of deep-bed, kinetics was used. At higher temperatures (in the 60 - 80°C range; see figure 7), the model simulated with an acceptable degree of accuracy the deep-bed drying process for various air conditions (inlet air temperature in the range of 60 - 90°C, inlet air velocity in the range of 0.7 - 2 $m.s^{-1}$) and bed heights (10 - 18 cm) (see figure 6). However at lower temperatures (*e.g.* 40°C), an overall underestimation of pellet mean moisture content was observed (see left sub-figure in figure 7). The mean absolute error was below 0.032 d.b. Using thin-layer kinetics, the product mass variation was the only experimental data available. During the drying process, though, heat and mass transfers are strongly coupled. Hence, identification using one or two datasets of deep-bed kinetics brings far more information (pellet mass variation, inlet and outlet air temperatures and relative humidities) and the identified parameters may be valid on a wider range of drying operating conditions. In addition, the identified D_{eff} parameters were also validated on classical drying-cooling operating conditions. Given the difficulties of recording drying-cooling kinetics, these results justify the decision to characterize formulations of animal feed pellets using only drying experiments.

5. Conclusion

Several formulations of pellets for animal feed were characterized experimentally and using correlations found in the literature. The sorption isotherms for all the different pellets yielded mostly similar results, close to those given previously by (Maier & Bakker-Arkema, 1992). The modified Henderson equation was preferred for numerical reasons and fitted onto the DVS data. To estimate the diffusion coefficient as a function of pellet moisture and temperature, several strategies were tested in the course of a larger project.

These were all based on inverse methods, i.e. to identify D_{eff} such that the simulated drying kinetics were as close as possible to experimental ones (identification set). With all parameters, the simulated drying kinetics, both in thin-layer and deep-bed arrangements, were in acceptable agreement with experimental ones (validation set), being close to the experimental uncertainties of the latter. Moreover, the model was proven to correctly simulate drying-cooling experiments. This approach is a possible workaround when dealing with the practical difficulties of performing reliable experiments on drying-cooling methods, especially at the thin-layer level. The same approach may be applied to different formulas of pellets with minimal laboratory work: measuring pellet size, adjusting the sorption isotherms (or neglecting their impact on the drying-cooling operation), and estimating the D_{eff} on the basis of a few experimental measurements of drying kinetics.

Current work in progress is focused on validation of the drying-cooling model at the industrial scale and the development of a user-friendly software sensor which can predict the final moisture content and temperature of pellets by comparing simulated and measured industrial data of outlet air temperature and humidity.

Acknowledgments

The authors wish to thank several undergraduate, Master's, and Ph.D. students (Perrine Leclercq, Analia Aparecida Vanzo, Abir Hosni, Azziz Zemmouri, Monica Pinto, and Benoit Hareng) for their valuable help in acquiring the experimental data that supported the modeling and simulation work. The authors wish to thank the French Agence Nationale de la Recherche (ANR) for the funding of the Ph.D. of C. Lambert, and the partners of the COOPERE-2 project, led by Veolia Research and Innovation, in collaboration with ProSim and ENSIACET. The authors also wish to thank the French Agency ADEME (Agence Nationale de l'Environnement et de la Maîtrise de l'Energie) for funding the experimental characterization and modeling of the drying of pellets.

References

Abud-Archila, M., Courtois, F., Bonazzi, C., & Bimbenet, J.-J. (2000). A compartmental model of thin layer drying kinetics of rough rice. *Drying Technology*, *18*, 1389–1414. URL: `http://www.tandfonline.com/doi/abs/10.1080/07373930008917784`. doi:`10.1080/07373930008917784`. `arXiv:http://www.tandfonline.com/doi/pdf/10.1080/07373930008917784`.

ASAE, S. (2007). D245.6. moisture relationships of plant-based agricultural products. *ASAE*, .

Bird, R. B., Stewart, W. E., & Lightfoot, E. N. (2002). Transport phenomena. Wiley and Sons.

de Blank, H., Hendrix, E., Litjens, M., & van Maaren, H. (1997). On-line control and optimisation of the pelleting process of animal feed. *Journal of the Science of Food and Agriculture*, *74*, 13–19. URL: http://dx.doi.org/10.1002/(SICI)1097-0010(199705)74:1<13::AID-JSFA755>3.0.CO;2-B. doi:10.1002/(SICI)1097-0010(199705)74:1<13::AID-JSFA755>3.0.CO;2-B.

Brook, R. C., & Foster, G. H. (1981). Handbook of transportation and marketing in agriculture. chapter Drying, cleaning and condtionning. (pp. 63–110). CRC Press Inc. volume II. Field Crops.

Chung, D. S., & Pfost, H. B. (1967). Adsorption and desorption of water vapor by cereal grains and their products. part i: Heat and free energy changes of adsorption and desorption. *Transactions of the ASAE*, *10*, 549–555.

Courtois, F. (1991). *Dynamic Modelling of Drying to Improve Processing Quality of Corn*. Ph.D. thesis ENSIA, Massy, France. URL: http://tel.archives-ouvertes.fr/tel-00308506/.

Galassi, M., Theiler, J., & Davies, J. (2009). Gnu scientific library reference manual. 3rd edition. Network Theory Ltd.

Hemmingsen, A. K. T., Stevik, A. M., Claussen, I. C., Lundblad, K. K., Prestlokken, E., Sorensen, M., & Eikevik, T. M. (2008). Water adsorption in feed ingredients for animal pellets at different temperatures, particle size, and ingredient combinations. *Drying Technology*, *26*, 738–748. doi:10.1080/07373930802046393.

Henderson, S. M. (1952). A basic concept of equilibrium moisture. *Agricultural Engineering*, *33*, 29–32.

Hill, C. A. S., Norton, A., & Newman, G. (2009). The water vapor sorption behavior of natural fibers. *Journal of Applied Polymer Science*, *112*, 1524–1537. URL: http://dx.doi.org/10.1002/app.29725. doi:10.1002/app.29725.

Kelley, R. L., Maier, D. E., & Bakker-Arkema, F. W. (1990). Evaluation of chilled cooling of feed pellets. *American Society of Agricultural Engineers*, *90*, 13.

Lambert, C., Goujot, D., Romdhana, H., & Courtois, F. (2015a). Toward a generic approach to build-up air drying models. *Drying Technology*, (p. 15). doi:10.1080/07373937.2015.1054510.

Lambert, C., Romdhana, H., & Courtois, F. (2015b). Reverse methodology to identify moisture diffusivity during air-drying of foodstuffs. *Drying Technology*, *33*, 1076–1085. URL:

http://dx.doi.org/10.1080/07373937.2014.985792. doi:10.1080/07373937.2014.985792. arXiv:http://dx.doi.org/10.1080/07373937.2014.985792.

Maier, D. E., & Bakker-Arkema, F. W. (1992). The counterflow cooling of feed pellets. *Journal of Agricultural Engineering Research*, *53*, 305–319. doi:10.1016/0021-8634(92)80089-B.

Maier, D. E., Kelley, R. L., & Bakker-Arkema, F. W. (1992). In-line, chilled air pellet cooling. *Feed Manage*, *43*, 28–32.

Nelder, J., & Mead, R. (1965). A simplex method for function minimization. *Computer Journal*, *7*, 308–313.

Sahin, S., & Sumnu, S. G. (2006). Physical properties of foods. (p. 257). Food Science.

Serena, A., & Bach Knudsen, K. E. (2007). Chemical and physicochemical characterisation of co-products from the vegetable food and agro industries. *Animal Feed Science and Technology*, *139*, 109–124. doi:10.1016/j.anifeedsci.2006.12.003.

Thomas, M., & van der Poel, A. (1996). Physical quality of pelleted animal feed 1: Criteria for pellet quality. *Animal Feed Science and Technology*, *61*, 89 – 112. URL: http://www.sciencedirect.com/science/article/pii/0377840196009492. doi:10.1016/0377-8401(96)00949-2.

Thomas, M., van Vliet, T., & van der Poel, A. (1998). Physical quality of pelleted animal feed 3. contribution of feedstuff components. *Animal Feed Science and Technology*, *70*, 59–78. URL: http://www.sciencedirect.com/science/article/pii/S0377840197000722. doi:10.1016/S0377-8401(97)00072-2.

Thomas, M., van Zuilichem, D., & van der Poel, A. (1997). Physical quality of pelleted animal feed. 2. contribution of processes and its conditions. *Animal Feed Science and Technology*, *64*, 173 – 192. URL: http://www.sciencedirect.com/science/article/pii/S0377840196010589. doi:10.1016/S0377-8401(96)01058-9.

Thompson, T. L. (1968). Mathematical simulation of corn drying: A new model. *Transactions of the American Society of Agricultural Engineers*, *24*, 582–586.

Wood, J. F. (1987). The functional properties of feed raw materials and their effect on the production and quality of feed pellets. *Animal Feed Science and Technology*, *18*, 1 – 17. URL: http://www.sciencedirect.com/science/article/pii/0377840187900253. doi:10.1016/0377-8401(87)90025-3.

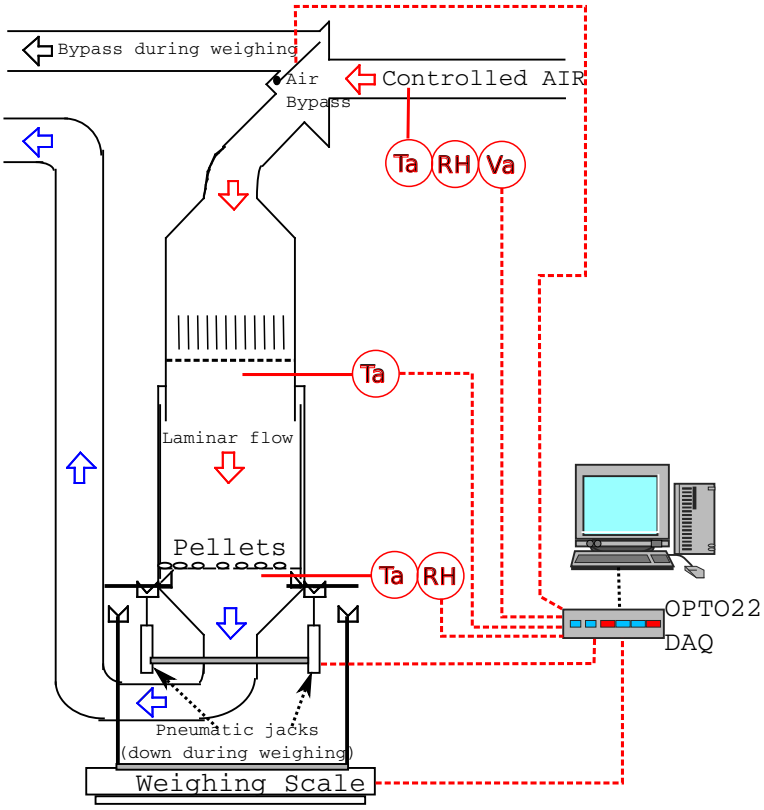

Figure 1: Schematic view of the drying pilot

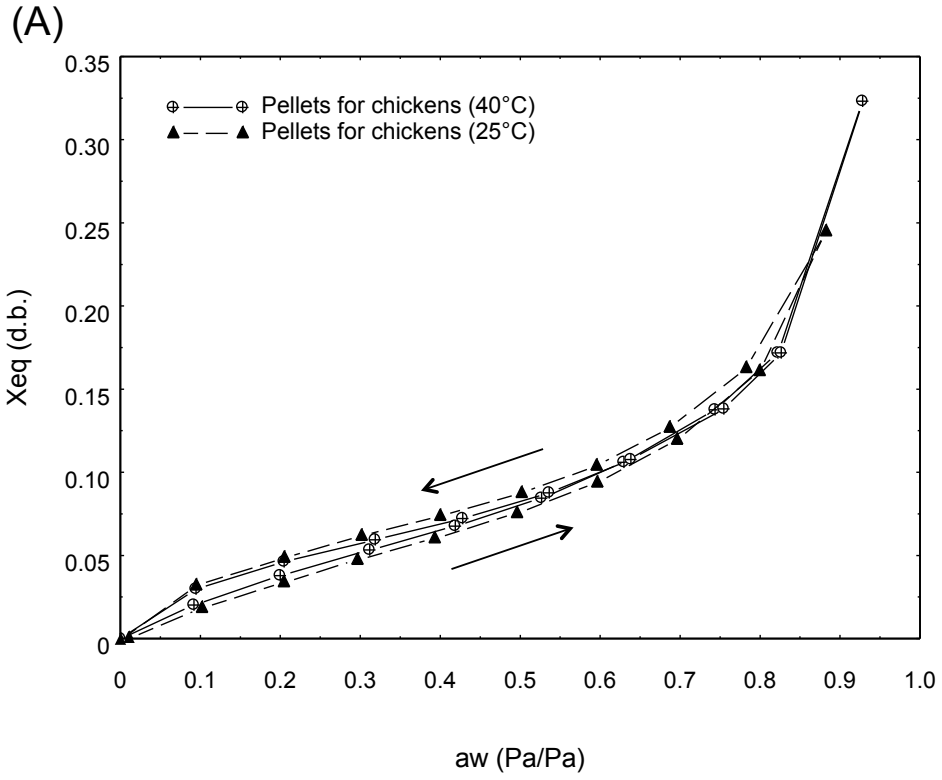

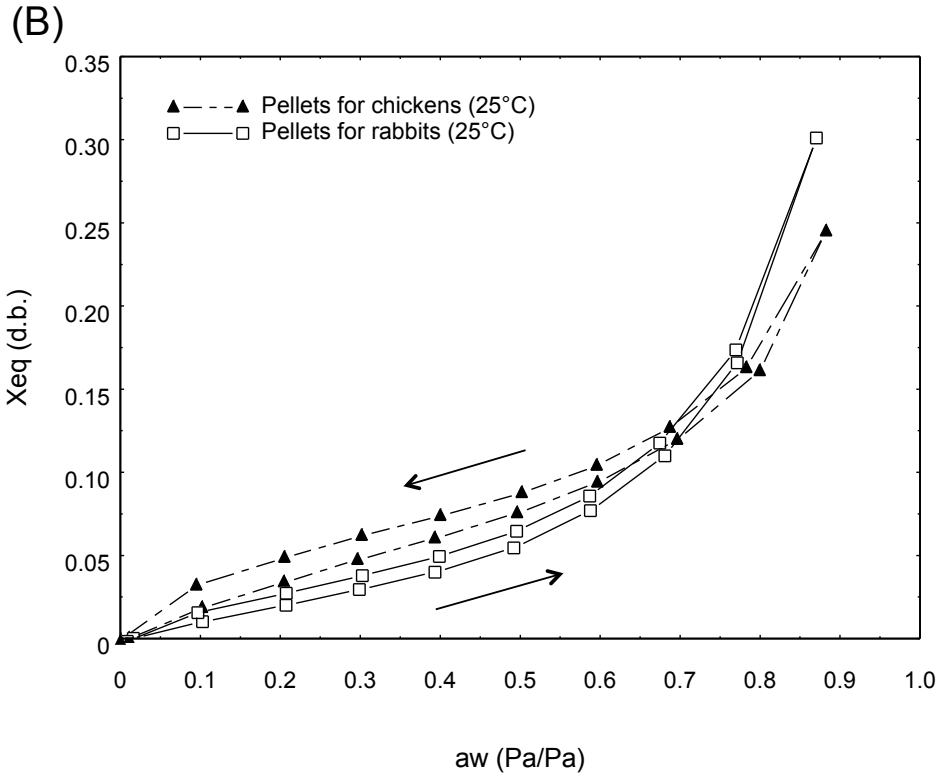

Figure 2: Sorption isotherms of pellets. (A) Effect of temperature on equilibrium moisture content, P4C pellets for chickens. (B) Effect of pellet formulation on equilibrium moisture content at 25°C. (→ adsorption curves), (← desorption curves).

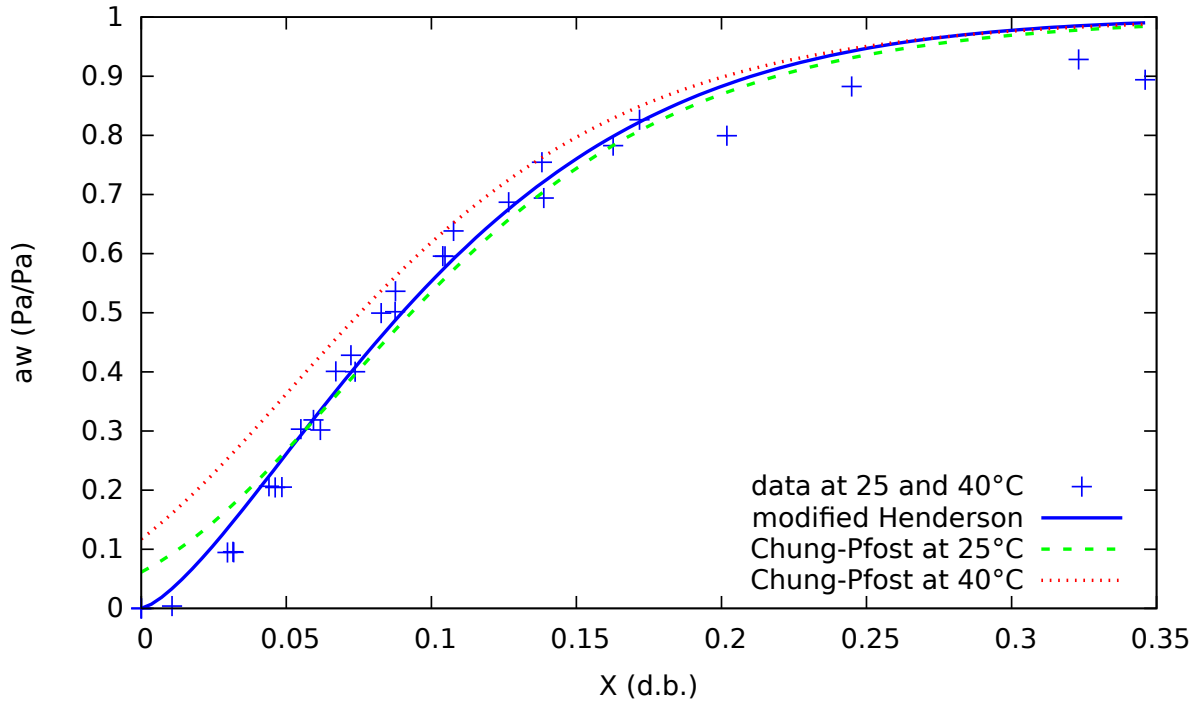

Figure 3: Fitting of sorption isotherms of pellets for rabbits (P4R - 4 mm) at 25°C and pellets for chickens (P4C) at 25°C and 40°C (+), with Henderson modified correlation (continuous line) (Henderson, 1952) and Chung-Pfost correlation (Chung & Pfost, 1967) at 25°C (dotted line) and 40°C (tiny dotted line).

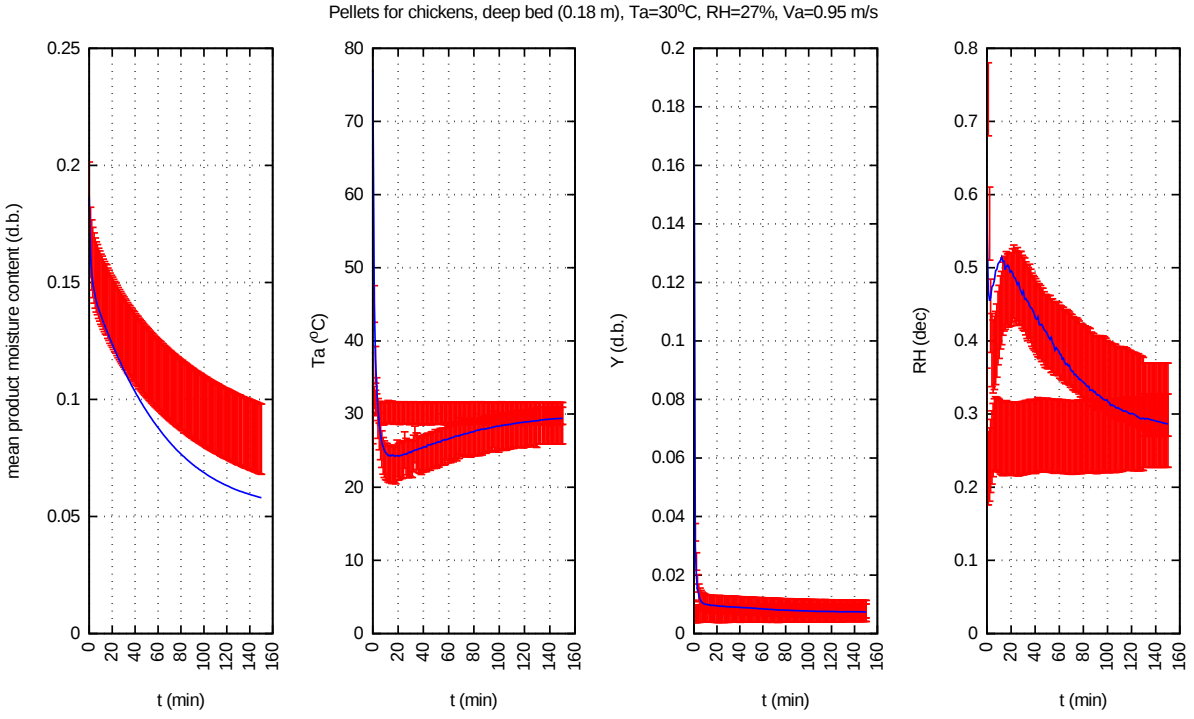

Figure 4: Comparison of experimental (dots with error bars) and simulated (-) data of deep-bed drying-cooling kinetics of pellets for chickens (validation set).

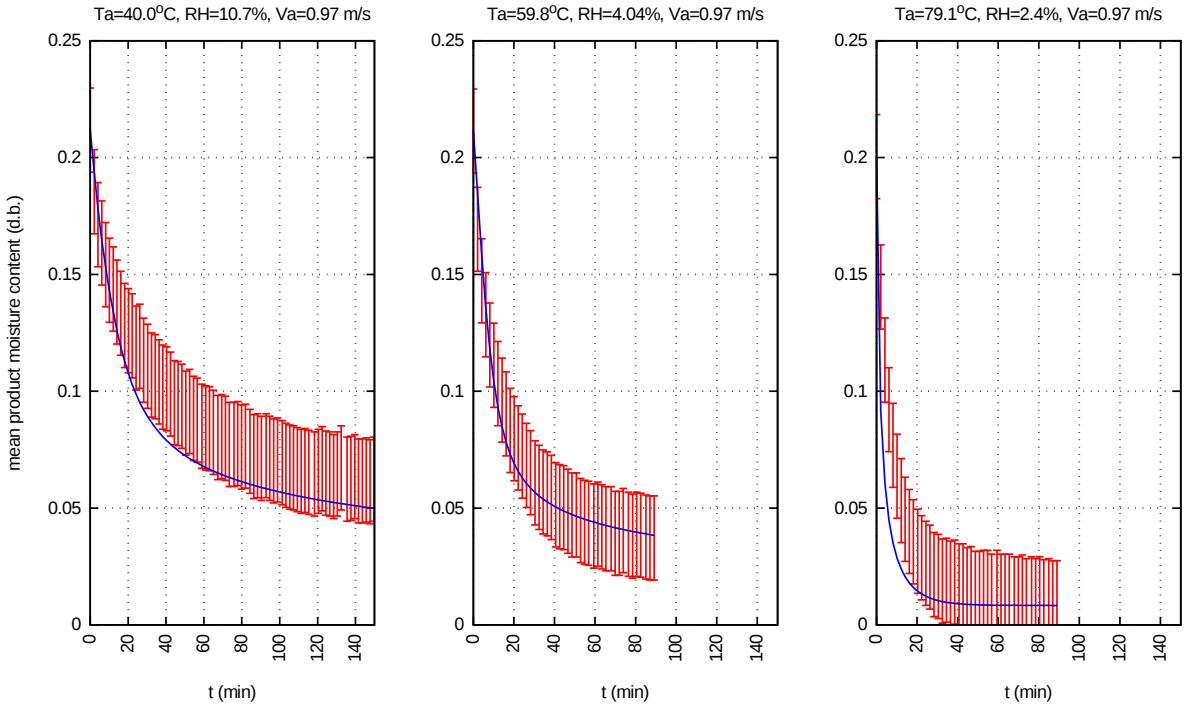

Figure 5: Comparison of experimental (dots with error bars) and simulated (-) data of thin-layer drying kinetics of the P4R - 4 mm pellets for rabbits (validation set)

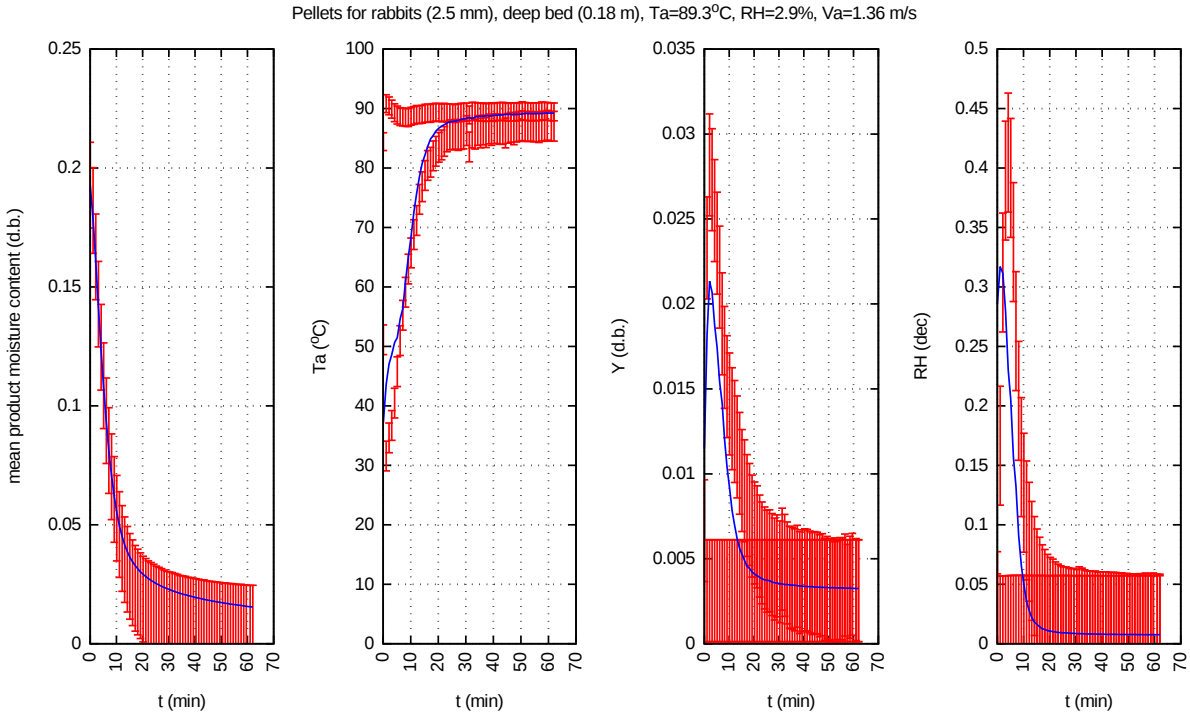

Figure 6: Comparison of experimental (dots with error bars) and simulated (-) data of deep-bed drying kinetics of the P4R - 2.5 mm pellets for rabbits (validation set)

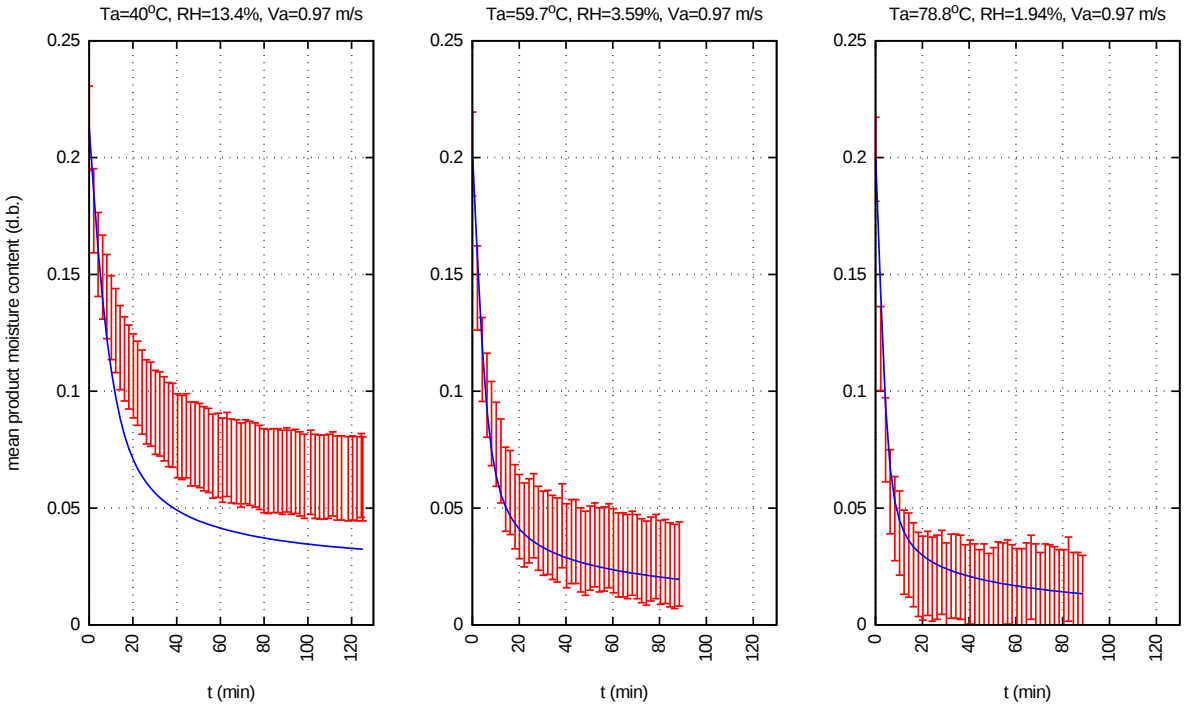

Figure 7: Comparison of experimental (dots with error bars) and simulated (-) data of thin-layer drying kinetics of the P4R - 2.5 mm pellets for rabbits (validation set)

Table 1: Composition of the pellets for chickens and rabbits (P4R - 2.5 mm and P4R - 4 mm)

Pellets for chickens		Pellets for rabbits	
Wheat	40 %	Wheat	4.5 %
Corn	20 %	Barley	13.2 %
Soybean cake	30 %	Soybean cake	5.8 %
Soybean seed	4 %	Soybean oil	0.5 %
Soybean oil	3 %	Grape pulp	5 %
Dicalcium phosphate	1.15 %	Sunflower cake	8.5 %
Calcium carbonate	0.95 %	Rape seed	3.5 %
Other	0.9 %	Milurex	8.5 %
		Cane molasses	6 %
		Sugar pulp	15 %
		Alfalfa	23.6 %
		Straw	3.5 %
		Calcium carbonate	0.9 %
		Other	1.5 %
Total	100 %	Total	100 %

Table 2: Dry matter composition of pellets for chickens and rabbits (P4R - 2.5 mm and P4R - 4 mm)

	Composition (% d.b.)	
	Pellets for chickens	Pellets for rabbits
Proteins	20.9	15.8
Lipids	19.1	3.9
Total sugar	54.5	70.5
Ashes	5.5	9.8

Table 3: Experimental conditions of the drying and the drying-cooling of pellets for chickens and rabbits

			Pellets for chickens	Pellets for rabbits
Drying kinetics	Thin layer experiments	Tp_0	$\approx$ 20 °C	$\approx$ 20 °C
		$\overline{X}_0$	0.204 d.b.	0.208 d.b.
		v_a	1 $m.s^{-1}$	1 $m.s^{-1}$
		Ta_0^0	30 - 90 °C	40 - 80 °C
	Deep bed experiments	height	$\approx$ 18 cm	10 - 18 cm
		Tp_0	$\approx$ 20 °C	$\approx$ 20 °C
		$\overline{\overline{X}}_0$	0.204 d.b.	0.208 d.b.
		v_a	1 $m.s^{-1}$	0.7 - 2.4 $m.s^{-1}$
		Ta_0^0	$\approx$ 90 °C	60 - 90 °C
Drying-cooling kinetics	Deep bed experiments	height	$\approx$ 18 cm	
		Tp_0	$\approx$ 60 °C	
		$\overline{\overline{X}}_0$	0.188 d.b.	
		v_a	1 $m.s^{-1}$	
		Ta_0^0	$\approx$ 30 °C	

$\overline{X_0}$, $\overline{\overline{X_0}}$ Initial mean moisture content of the pellets respectively in the case of thin layer and deep bed kinetics

Ta_0^0 Initial inlet air temperature

v_a Inlet air velocity

Tp_0 Initial temperature of the bed of pellets

Table 4: Strategies to identify effective moisture diffusivity of pellets for chickens and rabbits

	Pellets for chickens	**Pellets for rabbits (2.5 mm)**	**Pellets for rabbits (4 mm)**
Identification set	One set of deep bed kinetics (inlet air velocity fixed at 1 $m.s^{-1}$, inlet air temperature at 90 °C, and bed height at 18 cm)	Two thin layer kinetics (inlet air velocity fixed at 1 $m.s^{-1}$, inlet air temperature respectively at 40 and 80 °C)	Two deep bed kinetics (inlet air velocity fixed at 1 $m.s^{-1}$, inlet air temperature respectively at 60 and 80 °C, and bed height at 18 cm)
Validation set	All thin layer and drying-cooling kinetics	All other thin layer kinetics and deep bed kinetics	All thin layer kinetics

Table 5: Physical properties of pellets and parameters used in simulation

Property	Equation or value		
	Pellets for chickens	Pellets for rabbits ("2.5 mm")	Pellets for rabbits ("4 mm")
Radius	2.14 mm	0.95 mm	2.18 mm
Characteristic length	6.09 mm	6.14 mm	9.02 mm
Density	1,325 $kg.m^{-3}$	1,170 $kg.m^{-3}$	1,183 $kg.m^{-3}$
Porosity of the deep bed	0.56	0.58	0.56
Initial temperature		20 °C	
Initial moisture content	0.204 d.b.	0.211 d.b.	0.202 d.b.
Heat capacity	Choi and Okos correlation (Sahin & Sumnu, 2006)		
Thermal conductivity	Choi and Okos correlation (Sahin & Sumnu, 2006)		
Latent heat of vaporization	2.357 10^6 $J.Kg^{-1}$ (Courtois, 1991)		
Coefficient of heat transfer by convection	20 $W.m^{-2}.K^{-1}$		
Coefficient of mass transfer by convection	Lewis analogy		
Water activity	Modified Henderson correlation (Henderson, 1952)		
Effective moisture diffusivity	Abud correlation (Abud-Archila et al., 2000)		
Number of layer within the particle	10		
Height of the thin layer within the bed	1 mm		
Absolute tolerance	10^{-6}		
Relative tolerance	10^{-6}		
Initial time variation	10^{-3}		

Table 6: Identified values of effective moisture diffusivity for each formulation and geometry of pellets

	Pellets for chickens	Pellets for rabbits	
		P4R - 2.5 mm	P4R - 4 mm
d_1	22.153	25.177	26.694
d_2	0.2017	1.452	1.736

Table 7: Mean absolute errors observed on product mean moisture content and outlet air temperature of the kinetics of the validation set

		Mean absolute error		*Operating conditions of the kinetics of the validation set*			
		$\overline{X}$ *or* $\overline{\overline{X}}$ (d.b.)	Ta_{out} (°C)	Ta_{in} (°C)	v_a ($m.s^{-1}$)	*height* (cm)	Tp_0 (°C)
Pellets for chickens	TL	$<$ 0.016		30-70	1		20
	DC	0.022	0.8	30	1	18	60
P4R - 4 mm geometry of pellets for rabbits	TL	$<$ 0.012		40 - 80	1		20
P4R - 2.5 mm geometry of pellets for rabbits	TL	0.032 $<$ 0.014		40 60 - 80	1		20
	DB	$<$ 0.014	$<$ 4	60 - 90	0.7 - 2	10 - 18	20

TL Thin layer kinetics

DC Drying-cooling kinetics

DB Deep bed kinetics

$\overline{X}$ Mean moisture content of the particles (case of thin layer kinetics)

$\overline{\overline{X}}$ Mean moisture content of the particles within the bed (case of deep bed kinetics)

Ta_{out} Outlet air temperature

Ta_{in} Inlet air temperature

v_a Inlet air velocity

Tp_0 Initial temperature of the bed of pellets